

Translational and rotational dynamics of water in mesoporous silica materials: MCM-41-S and MCM-48-S

Antonio Faraone

Department of Nuclear Engineering, Massachusetts Institute of Technology, Cambridge, Massachusetts and Department of Physics and INFN, University of Messina, Messina, Italy

Li Liu

Department of Nuclear Engineering, Massachusetts Institute of Technology, Cambridge, Massachusetts

Chung-Yuan Mou and Pei-Chun Shih

Department of Chemistry, National Taiwan University, Taipei, Taiwan

John R. D. Copley

National Institute of Standards and Technology Center for Neutron Research, Gaithersburg, Maryland

Sow-Hsin Chen^{a)}

Department of Nuclear Engineering, Massachusetts Institute of Technology, Cambridge, Massachusetts

(Received 25 March 2003; accepted 30 April 2003)

We investigated the translational and rotational dynamics of water molecules in mesoporous silica materials MCM-41-S and MCM-48-S using the incoherent quasielastic neutron scattering technique. The range of wave vector transfers Q covered in the measurements was from 0.27 to 1.93 \AA^{-1} broad enough to detect both the translational and rotational contributions to the scattering. We used the relaxing-cage models for both translational and rotational motions which we developed earlier, to analyze the QENS spectra and investigated water dynamics in a supercooled range from 250 to 280 K. The results show a marked slowing down of both the translational and rotational relaxation times, and an increasing effect of confinement on the translational motion, as the temperature is lowered. © 2003 American Institute of Physics. [DOI: 10.1063/1.1584653]

I. INTRODUCTION

Water in confinement has been extensively studied both theoretically and experimentally, because it is believed to strongly affect the properties of the systems in which it is dispersed, in small nano-sized pores or cavities. However, the microscopic mechanism of diffusion and rotation of a water molecule near a hydrophilic surface at supercooled temperatures is still not fully understood. In the past, we have studied the translational dynamics of water confined in pores of Vycor glass using the translational relaxing-cage model.¹ One problem with Vycor glass is that the pores have a broad size distribution, and the average pore diameter of 50 \AA is too large to show all the effects of confinement. For this reason, we collected new quasielastic neutron scattering (QENS) data on water confined in lab-synthesized mesoporous glasses MCM-41-S and MCM-48-S. In comparison with Vycor glass, these molecular sieves have smaller pores with a narrower size distribution. Moreover, MCM-41-S and MCM-48-S allow us to study dynamical effects of different pore morphologies; the former matrix (25 \AA pore diameter) has 1D cylindrical tubes arranged in a hexagonal structure, whereas MCM-48-S (22 \AA pore diameter) has 3D bicontinuous morphology.

The QENS technique is particularly suitable for studying single particle dynamics of water molecules because of the very high incoherent scattering cross section of hydrogen

atoms as compared to that of oxygen atoms. Moreover, QENS spectra are sensitive to both translational and rotational dynamics of the typical water molecule. To get correct information it is very important to analyze the data using a realistic model. In this respect, comparison of the model of the analysis with molecular dynamics (MD) simulations of water has been extremely helpful. In fact, using MD calculated trajectories it is possible to obtain simulated dynamical quantities, such as the intermediate scattering function (ISF) of the hydrogen atom, and of the center of mass of the water molecule, with good accuracy. With the help of MD data generated with the extended simple charge model (SPC/E) of water, we developed the relaxing cage models (RCM) for both the translational and rotational motions,^{2,3} borrowing concepts derived from mode coupling theory (MCT). The models take into account the characteristic properties of short-time dynamics of water and reproduce both MD and experimental results very well.

In this paper we report the results of our analyses of QENS data of water confined in the MCM-41-S and MCM-48-S matrices according to the RCM. Using a realistic model, we have been able to extract the temperature dependence of the average translational and rotational relaxation times of water. By using silica matrices having pore dimensions much smaller than that of Vycor glass, we have been able to detect a strong effect of confinement on both the

^{a)}Electronic mail: sowhsin@mit.edu

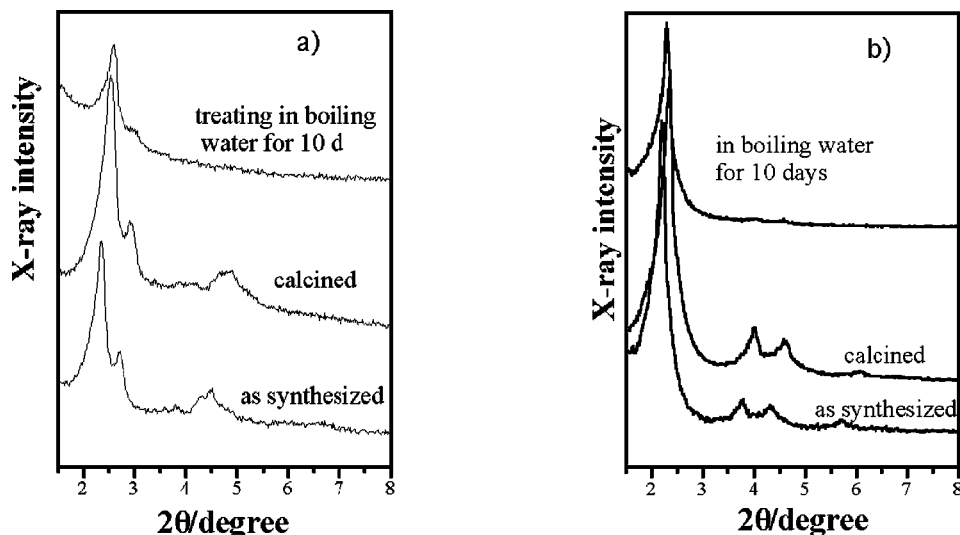


FIG. 1. The XRD patterns of (a) MCM-48-S (pcb-072c), (b) MCM-41-S (pcb-159c).

translational and rotational dynamics of water molecules. Moreover, analyzing the Q dependence of the spectra, we investigated the space-time characteristic of the long-time diffusive process, in particular its dimensionality.

II. EXPERIMENT

A. Sample preparation

To synthesize the MCM samples, zeolite seeds were prepared by mixing NaAlO_2 (Riedel-de Haen), NaOH (Shimadzu's Pure Chemicals, Japan), fumed silica (Sigma), tetraethyl ammonium hydroxide (TEAOH) aqueous solution (20%) (Acros), and water under stirring for 2 to 5 h, then placing the solution in an autoclave at 100°C for 18 h. A clear solution of nanoprecursors was obtained. MCM-48-S (pcb-072c)⁴ was synthesized by reacting zeolite seeds with cetyltrimethylammonium bromide solution (CTAB, Acros) at 150°C for 6 to 24 h. Samples were then collected by filtration, washed with water, dried at 100°C in an oven for 6 h, and calcined at 580°C for 6 h. To obtain MCM-41-S (pcb-159c)⁵ the mixture of zeolite seeds and surfactant solution was hydrothermally treated at 150°C for 2 to 6 h, creating a disordered mesostructure. After pH adjustment and hydrothermal reaction at 100°C for 2 days, we obtained the desired mesoporous material. In both cases the molar ratios of the reactants NaAlO_2 : SiO_2 : NaOH : TEAOH : C_{16}TMAB : H_2O were 1:37–67:1.5–9:11–22:18.3:3000–3500. Using x-ray diffraction (XRD) experiments we found that the MCM-48-S was well ordered with cubic (Ia3d) symmetry, whereas the MCM-41-S had hexagonal (P6mm) symmetry, as shown in Fig. 1. Pore diameters were determined using a nitrogen adsorption technique. Both samples exhibit high hydrothermal stability. In order to hydrate the mesoporous matrices we put the calcined samples to the diskette that was full of water vapor by pumping the saturated NaCl solution for 2 to 3 days. We thus obtained water-loaded samples with hydration levels ($\text{gr}_{\text{H}_2\text{O}}/\text{gr}_{\text{sample}}$) of $\approx 35\%$ (pcb-072c) and $\approx 30\%$ (pcb-159c). The amount of loading was determined by thermogravimetric analysis. For the QENS experiments the hydrated powder was evenly spread

to form a rectangular slab sample 0.5 mm thick, such that multiple-scattering corrections should not be necessary (transmission 95%).

B. QENS experiment

The QENS measurements were carried out at the NIST Center for Neutron Research, using the disk chopper spectrometer (DCS⁶). The incident neutron wavelength was 6.0 \AA and the energy resolution full width at half maximum (FWHM) was $\sim 30 \mu\text{eV}$. The rectangular sample cell was placed at 45° to the direction of the incident neutron beam. The detectors facing the edge of the can have been discarded. The data were grouped to obtain two sets of three and six constant angle spectra, in transmission geometry, at low scattering angles, and in reflection geometry, at high scattering angles, respectively. The resulting range of elastic wave-vector transfers Q was from 0.27 to 1.93 \AA^{-1} . The time-of-flight spectra were corrected for scattering from the same sample holder, standardized using results from a run using vanadium, and converted to the differential scattering cross section using standard routines available at NIST.

III. THEORETICAL BACKGROUND

In Fig. 2 we give, as an example, the experimental spectrum, together with the results of the fit and the fit components, for a MCM-48-S hydrated sample at $T=270 \text{ K}$, at $Q=1.93 \text{ \AA}^{-1}$. This figure is a good example of the general quality of the fit.

As shown in Fig. 2, we detect an elastic component in the spectra. This contribution is due to the scattering of the silica matrix, in which a small number of hydrogen atoms from the residual unburned template is present. Moreover, QENS experiments on partially hydrated silica matrices^{1,7,8} and molecular dynamics simulations⁹ have shown that the layer of water near the surface of the pores has a dynamic that is much slower than that of the water molecules in the inner part of the pores. Thus, it is possible that a fraction of the water molecules in the pores, likely on the hydrophilic surface, has a dynamic which is too slow to be resolved

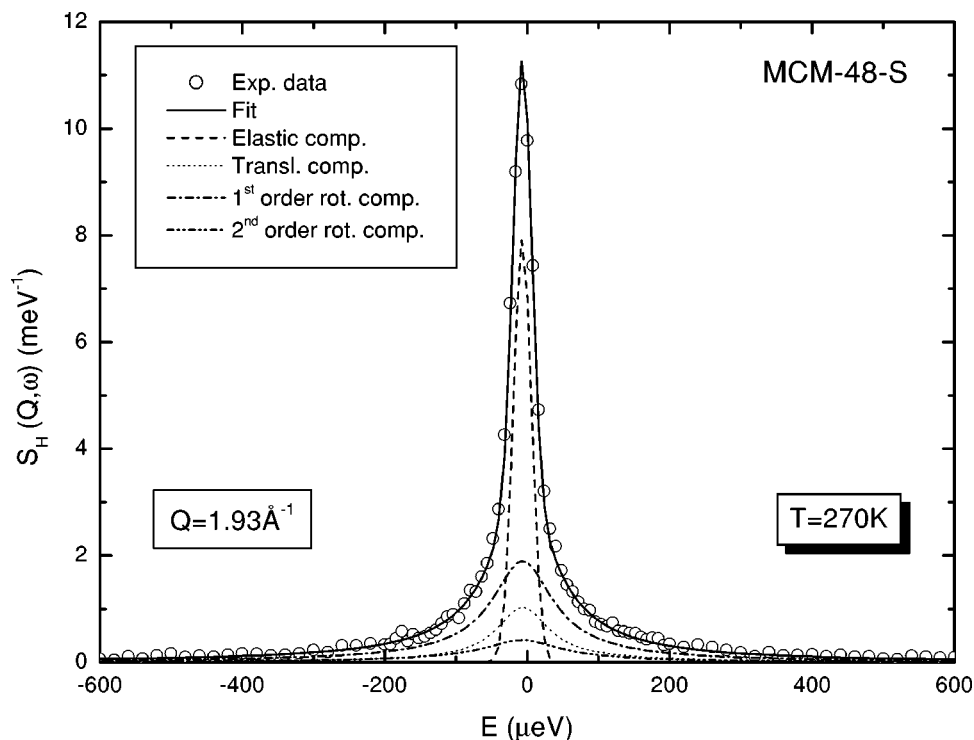


FIG. 2. A typical QENS spectrum from a MCM-48-S hydrated sample at $T=270$ K, at $Q=1.93 \text{ \AA}^{-1}$. The errors are no larger than the symbols. The continuous line represents the result of the fit; the dashed line is the elastic component; the dotted, dash-dot, and dash-dot-dot lines represent contributions to the scattering from the first three terms of the Sears expansion.

using the $30 \mu\text{eV}$ resolution of DCS. The scattering originating from these molecules is elastic. The remaining, quasi-elastic, part of the spectra is due to the incoherent scattering from the remaining water molecules. We used the RCM to describe the dynamics of these water molecules. This model has already been tested against MD simulations^{2,3} and QENS experiments.^{1,10,11} The model has been developed using MD data from supercooled water. Since the dynamics of water confined in small pores or on the surface of big particles is supposed to be similar to that of supercooled water,¹² the model has been successfully used to analyze neutron scattering data from water confined in a nanoporous matrix and in cement paste. Thus, we write

$$S(Q, \omega) = pR(Q_0, \omega) + (1-p)FT\{F_H(Q, t)R(Q_0, t)\}, \quad (1)$$

where $F_H(Q, t)$ is the hydrogen atoms' ISF, p is the area of the elastic component, $E = \hbar\omega$ is the energy transfer of the neutron, and Q is the magnitude of the wave-vector transfer corresponding to this energy transfer and to the scattering angle θ . The elastic Q value is given by $Q_0 = [4\pi \sin(\theta/2)]/\lambda$. $R(Q_0, t)$ is the Fourier transform of the experimental resolution function, $R(Q_0, \omega)$.

For Q values larger than $\approx 1 \text{ \AA}^{-1}$, the spectrum is determined by both the translational and rotational dynamics of water molecules. Following the indications of our previous MD^{3,13} simulations, we used the decoupling approximation, $F_H(Q, t) = F_T(Q, t) \cdot F_R(Q, t)$, $F_T(Q, t)$ and $F_R(Q, t)$ being the translational and rotational ISFs, respectively. This approximation is based on the assumption of the statistical independence of the translational and rotational motions. However, this assumption has been criticized in the past,¹⁴ and it has been shown to be unrealistic. It has also been suggested that the long-time decay of the hydrogen atoms ISF can be approximated by the center-of-mass ISF.¹³ This approxima-

tion is good especially at low Q ; however, it is less and less accurate at $Q \geq 1 \text{ \AA}^{-1}$. Our recent MD results³ of 216 SPC/E water molecules (the details of the MD simulations and potential are reported in the Appendix) have shown that the decoupling approximation is accurate within 10 %, as shown in Fig. 3. Such precision is acceptable when dealing with experimental QENS data. It is important to underline that the decoupling approximation is the best way to account for the effects of rotations on neutron spectra and to extract information on the rotational dynamics.

According to the RCM the translational dynamics of water is expressed as the product of a short-time harmonic motion and a long-time decay. In fact, at supercooled temperatures, at short times, a water molecule is trapped inside the cage of its neighbors. Inside this cage the translational motion of the molecule is harmonic. At long times eventually the cage breaks and the water molecule diffuses away. This process involves the structural relaxation of the cage and cannot be described by a simple Debye process. This α -relaxation-like process must be described using a stretched exponential. Thus, we write

$$F_T(Q, t) = F_T^s(Q, t) \exp[-(t/\tau_T)^\beta]. \quad (2)$$

The first term describes the rattling motion of the molecule inside the cage of its neighbors using a Gaussian term²

$$F_T^s(Q, t) = \exp\left\{-Q^2 v_0^2 \left[\frac{1-C}{\omega_1^2} (1 - e^{-\omega_1^2 t^2/2}) + \frac{C}{\omega_2^2} (1 - e^{-\omega_2^2 t^2/2}) \right]\right\}. \quad (3)$$

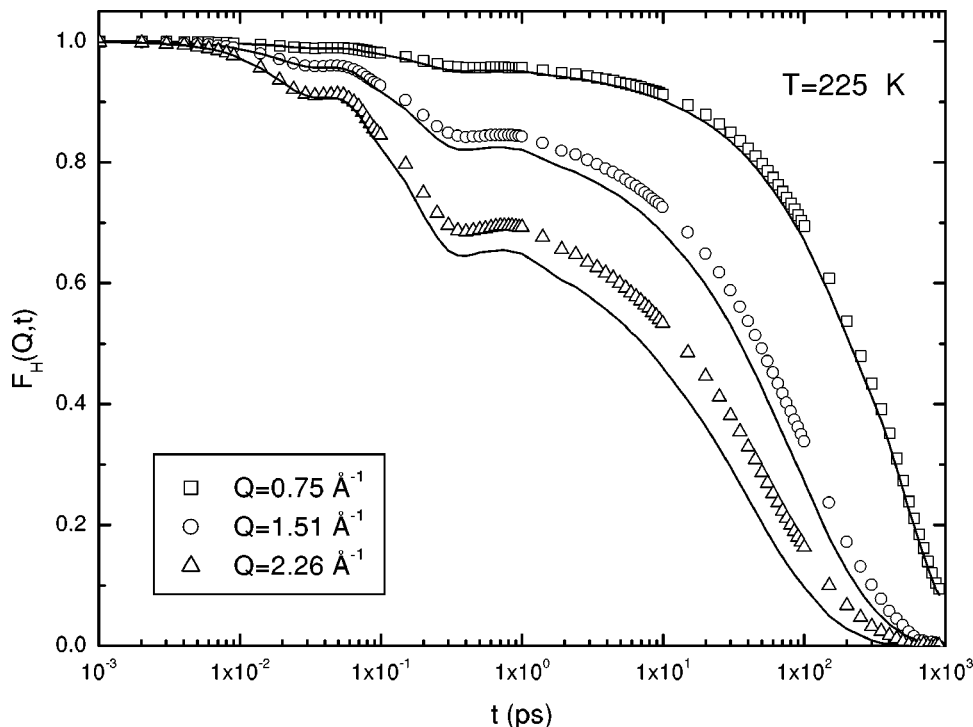


FIG. 3. The intermediate scattering functions from MD simulations of 216 SPC/E water molecules, at three Q values (0.75, 1.51, and 2.26 \AA^{-1}) and at $T=225 \text{ K}$ (Ref. 3). The open symbols represent $F_H(Q,t)$; the lines represent the decoupling approximation results: $F_T(Q,t) \cdot F_R(Q,t)$.

In this equation $v_0 = \sqrt{k_B T/m}$ is the thermal speed of the water molecule, $\sqrt{2}\omega_1 \approx 15.3 \text{ THz}$ (8 meV) and $\sqrt{2}\omega_2 \approx 59.4 \text{ THz}$ (30 meV) are the peak frequencies of the translational density of states, $Z_T(\omega)$, of the hydrogen atom, and C expresses their relative weights. This expression has been determined through the analysis of MD simulated $Z_T(\omega)$, which agrees with previous inelastic neutron scattering (INS) experiment.⁸ This analysis yields the values $\omega_1 = 10.8 \text{ THz}$, $\omega_2 = 42.0 \text{ THz}$, and $C = 0.44$.

The long-time dynamics is characterized by a structural relaxation time, τ_T , that both experiments and MD simulations have shown to follow a power law in Q , namely, $\tau_T = \tau_0(aQ)^{-\gamma}$.^{1,2,7} Here, a is a suitable length scale, the root-mean-square vibrational amplitude of water rattling inside the cage, defined by the long-time limit of $F_T^s(Q,t)$. According to MD simulations $a = 0.5 \text{ \AA}$, and is fairly insensitive to temperature variations.² The exponent γ is 2 for simple diffusion. MD results² suggest that in supercooled water γ is Q dependent, being 2 in the hydrodynamic limit ($Q \rightarrow 0$), decreasing to a plateau value (≤ 2) at $Q < 1.0 \text{ \AA}^{-1}$. However, experimentally it is very difficult to appreciate the Q dependence of γ since a log-log plot of τ_T versus Q gives a straight line within experimental uncertainties, as found in many QENS studies on confined water.^{1,7} The stretch exponent β is Q dependent according to MD results,² being 1 at $Q=0$, and decreasing with Q . However, the analysis of QENS spectra furnishes values of β almost constant with Q ^{10,11} in the investigated range. Thus, we assumed that both γ and β are Q independent.

As far as the rotational contribution is concerned, the Q and t dependence of $F_R(Q,t)$ can be separated using the well-known Sears expansion¹⁵

$$F_R(Q,t) = \sum_{l=0}^{\infty} (2l+1) j_l^2(Qb) C_l(t), \quad (4)$$

where j_l is the spherical Bessel function of order l , and $C_l(t)$ is the l th-order rotational correlation function. Since the center of mass to hydrogen atom distance in water is well known, $b = 0.98 \text{ \AA}$, the Q dependence of the rotational ISF is fully determined.

At short times, because of the cage effect, a water molecule can only perform harmonic librations; at long times, when the cage breaks, it can rotate freely, losing memory of its original orientation. Thus, like the translational ISF, the first-order rotational correlation function has been shown³ to be describable as the product of a short-time vibrational part and a long-time decay

$$C_1(t) = C_1^s(t) \exp[-(t/\tau_R)^\beta]. \quad (5)$$

The short-time rotational dynamic is given by³

$$C_1^s(t) = \exp \left\{ -\frac{4\langle \omega^2 \rangle}{45\omega_3^2} [3(1 - e^{-\omega_3^2 t^2/2}) + 6\omega_3^2 t^2 e^{-\omega_3^2 t^2/2} - \omega_3^4 t^4 e^{-\omega_3^2 t^2/2}] \right\}, \quad (6)$$

where $\langle \omega^2 \rangle$ is the mean-square angular velocity, related to the effective moment of inertia of the water molecule in the cage, and $\sqrt{6}\omega_3 \approx 65 \text{ meV}$ the characteristic frequency of hindered rotations around the H-bond direction.⁸ It is well known that the hindered rotations of the water molecules contribute to the INS spectra with a band composed of three peaks corresponding to the rotations around the three axes of

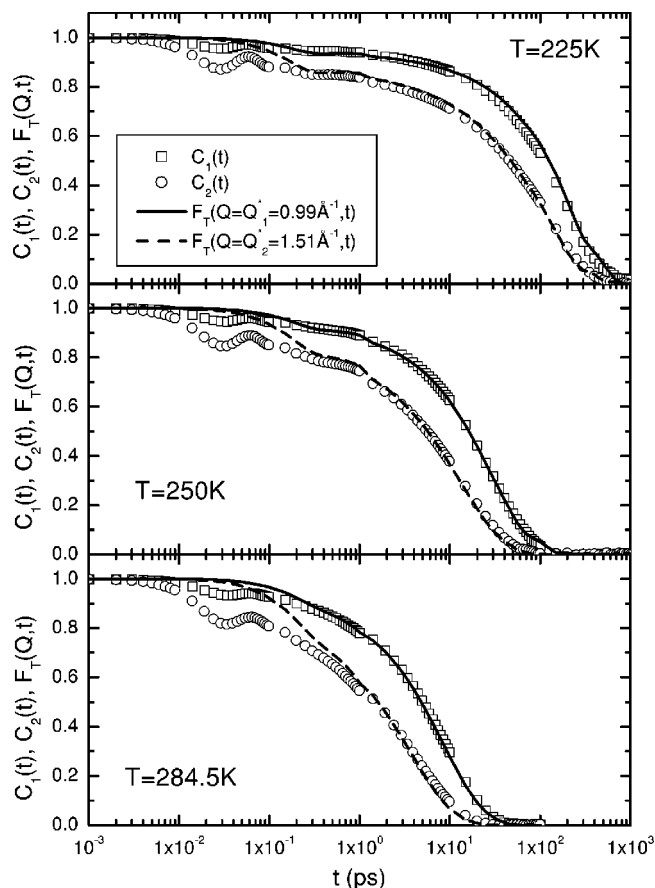


FIG. 4. The translational ISF at $Q=0.99 \text{ \AA}^{-1}$ (solid lines) and $Q=1.51 \text{ \AA}^{-1}$ (dashed lines), the first- (open squares) and second- (open circles) order rotational correlation functions as calculated from MD simulations of 1000 SPC/E water molecules, at $T=225, 250,$ and 284.5 K . The figure shows that the long-time behavior of $F_T(Q=0.99 \text{ \AA}^{-1}, t)$ coincides with the long-time behavior of $C_1(t)$ for all the investigated temperatures. In the same way, the long-time behavior of $F_T(Q=1.51 \text{ \AA}^{-1}, t)$ coincides with the long-time behavior of $C_2(t)$ for all the investigated temperatures.

the molecule. However, the pseudo-Gaussian expression reported in Eq. (6) is able to describe this band fairly.³

MD results¹⁶ put in evidence that the long-time translational and rotational motions are strongly coupled, both being connected to the diffusion outside the cage. This occurrence is clearly shown by the fact that the long-time part of $C_1(t)$ coincides with the translational ISF at a certain Q^* value, T independent, as shown in Fig. 4. Figure 4 shows that the long-time behavior of $F_T(Q=0.99 \text{ \AA}^{-1}, t)$ and $F_T(Q=1.51 \text{ \AA}^{-1}, t)$ coincides with the long-time behavior of $C_1(t)$ and $C_2(t)$, respectively, for all the investigated temperatures, in our MD simulations of 1000 SPC/E water molecules. In order to ensure that our model accounts for this coupling we used the same stretch exponent, β , for both the translational and rotational dynamics. Then, by imposing the equality $\tau_T(Q^*) = \tau_R$, we were able to determine Q^* . Unfortunately, the decoupling approximation neglects any coupling between the translational and rotational motion. Thus, the model does not exactly reproduce the ISF. The higher order rotational correlation functions are then generated from $C_1(t)$ using the maximum entropy method.¹⁷ The distribution function of the water molecules' orientation, with re-

spect to their initial orientation, is determined by maximizing the information entropy of the distribution, under the constraints that the distribution is positive, normalized, and gives the correct, known, first-order rotational correlation function, $C_1(t)$. Thus, the higher order rotational correlation functions can be calculated using the distribution function determined this way. This method is very effective at short times and allows us to get $F_R(Q, t)$ in good agreement with the simulated result in the $0 < Q \leq 2$ range.³

The model contains four parameters, namely C , ω_1 , ω_2 , and ω_3 , describing the short-time dynamics of the molecule. These parameters are better determined from the analysis of the inelastic part of the spectrum, and are insensitive to small temperature variations. For this reason we have fixed their values according to the results of our MD simulations, which agree with previous inelastic neutron scattering measurements.⁸ The remaining parameters, namely p , τ_0 , γ , $\langle \omega^2 \rangle$, τ_R , and β , can be determined from the analysis of the QENS spectra. Since they are Q independent, we fit the experimental $S(Q, \omega)$ surface (both ω - and Q -dependence) using just six fitting parameters. We took into account the first three terms of the Sears expansion. This procedure succeeded when applied to water in hydrated cement paste.¹¹ The quality of the fit reported in Fig. 2 shows that the model describes the experimental spectra with good accuracy. In Fig. 5 we show the fit results for both the samples at three different Q values in the low, intermediate, and high Q region, respectively. The quality of the spectra ensures that using only six fitting parameters we were able to reproduce the spectra for all the investigated Q values (nine spectra).

IV. RESULTS AND DISCUSSION

In Table I we report the numerical values obtained for the fitting parameters for both the matrices at all the investigated temperatures. In Fig. 6 we show the parameters p , β , and γ extracted from the fitting process, as a function of temperature. In plot (a) we report the weight of the elastic contribution to the spectra, p . As previously stated, this fraction includes both the contributions from the silica matrix and from water molecules, likely close to the pore surface, whose dynamics is too slow to be detected with the $30 \mu\text{eV}$ resolution of DCS. We have performed additional measurements at higher temperatures using the Fermi chopper spectrometer (FCS) at NIST.¹⁸ These measurements clearly show that at higher temperatures p reaches the limiting values (about 10%) shown in Fig. 6(a). We identify this value with the elastic scattering from the silica matrix. The remaining elastic contribution comes from water molecules whose dynamic is much slower than that of the other water molecules. The number of these molecules increases with decreasing temperature. In the case of MCM-48-S, having smaller pores, the increase is much faster.

In Fig. 6(b) we show the stretch exponent β . The translational and rotational relaxation processes are not exponential. Their value decreases with temperature. This finding could be a property of water dynamics; however, it could also be due to the nonzero resolution of the instrument that, as the dynamic slows down, is not able to fully resolve the non-Lorentzian feature of the spectra. We think the reason-

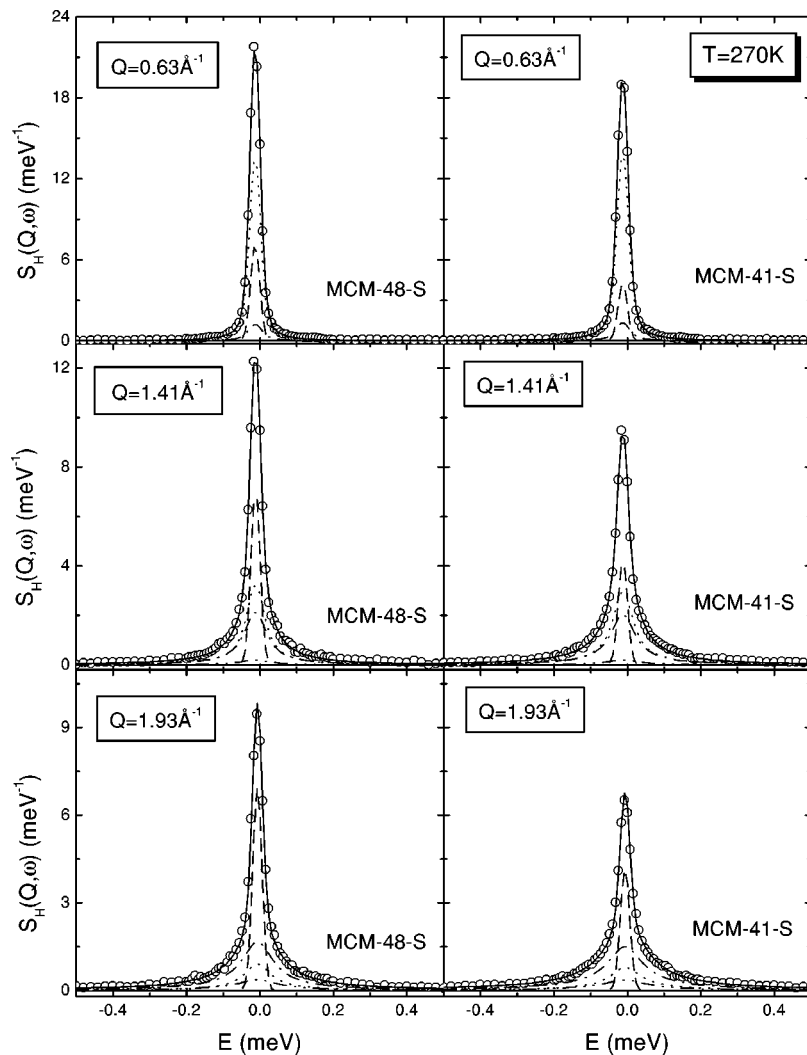


FIG. 5. Typical QENS spectra from an MCM-41-S and an MCM-48-S sample at $T=270$ K at three different Q values. The errors are no larger than the symbols. The continuous line represents the result of the fit; the dashed line is the elastic component; the dotted, dash-dot, and dash-dot-dot lines represent contributions to the scattering from the first three terms of the Sears expansion.

able value of β is about 0.75 for both matrices independent of temperature in the measured temperature range.

Confinement affects the translational dynamic of water in many ways. It lowers the freezing point, allowing the study of deeply supercooled states and, on the other hand, it slows down the dynamics of the water molecules. Moreover, it has an interesting effect on the dimensionality of the diffusion process. The diffusive relaxation time usually scales with Q^2 , but in Fig. 6(c), we find that $\gamma < 2$ at low tempera-

ture and slowly increases, reaching the diffusive value at higher temperatures. The value of γ is lower in MCM-48-S than in MCM-41-S. However, more data are necessary to address the question whether the behavior of γ is mostly influenced by the morphology of the pores, or by their sizes.

From Eq. (2), it can be seen that if the product $\beta\gamma$ is equal 2, $F_T(Q, t)$ has a Gaussian form with respect to Q . In this case, the van Hove self-correlation function of the center of mass is Gaussian as well. We have found $\beta\gamma < 2$, indicat-

TABLE I. Numerical values of the extracted fitting parameters.

T (K)	p	τ_0 (ps)	τ_R (ps)	β	γ
MCM-48-S					
250	0.47 ± 0.02	21.7 ± 5.4	193.5 ± 107.3	0.94 ± 0.07	1.67 ± 0.18
260	0.31 ± 0.02	17.2 ± 3.5	120.8 ± 47.4	0.87 ± 0.07	1.72 ± 0.14
270	0.22 ± 0.01	11.0 ± 0.8	91.8 ± 2.7	0.78 ± 0.01	1.89 ± 0.03
280	0.18 ± 0.02	7.5 ± 0.7	42.6 ± 0.3	0.75 ± 0.03	1.96 ± 0.12
MCM-41-S					
250	0.25 ± 0.02	16.4 ± 2.8	190.3 ± 55.1	0.83 ± 0.06	1.82 ± 0.14
260	0.18 ± 0.01	11.3 ± 1.5	166.4 ± 3.2	0.78 ± 0.01	1.94 ± 0.10
270	0.13 ± 0.01	8.0 ± 0.9	119.6 ± 11.1	0.74 ± 0.06	2.00 ± 0.12
280	0.10 ± 0.02	6.2 ± 0.6	35.1 ± 0.3	0.72 ± 0.08	2.00 ± 0.13

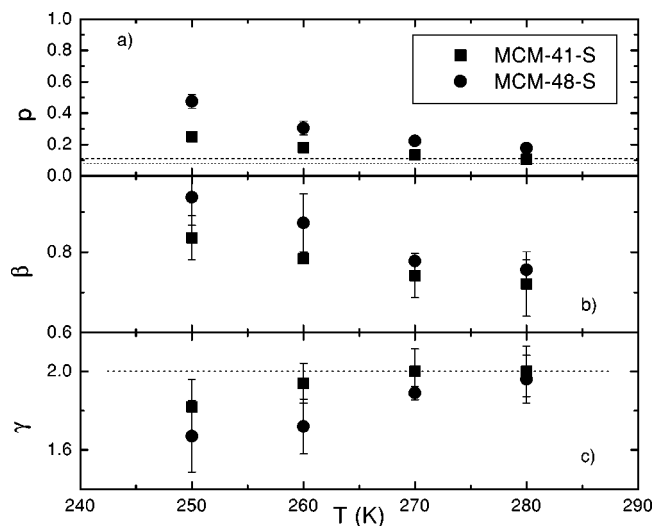


FIG. 6. Temperature dependence of the fitting parameters p , β , and γ . In plot (a) dashed and dotted lines represent the scattering contribution from the matrix for MCM-41-S and MCM-48-S, respectively. In plot (c) the dotted lines represent the limiting diffusion value of the parameter γ .

ing that the Gaussian approximation is not valid for water in MCM at supercooled temperatures. This finding is in agreement with previous MD simulations¹⁹ of supercooled water, which have shown the breakdown of the Gaussian approximation in the long-time region.

In Fig. 7(a) we show the temperature dependence of the average translational relaxation time, $\langle\tau_0\rangle = (\tau_0/\beta)\Gamma(1/\beta)$. As expected, it increases with decreasing temperature for both samples. Larger values are obtained in the MCM-48-S sample, although within experimental uncertainty. This is probably due to the fact that the pores of this sample are slightly smaller. This occurrence does not seem to affect the rotational dynamics. In fact, the extracted average rotational relaxation times, $\langle\tau_R\rangle = (\tau_R/\beta)\Gamma(1/\beta)$, can hardly be considered different for the two samples. The rotation process of a water molecule takes place within a

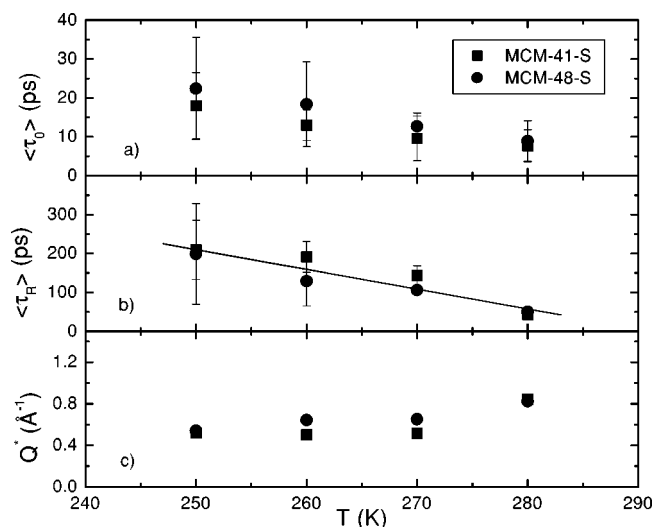


FIG. 7. Temperature behavior of the parameters $\langle\tau_0\rangle$, $\langle\tau_R\rangle$, and Q^* , as determined from the results of the fitting procedure. In plot (b) the continuous line represents a linear fit to the eight points.

sphere of radius b from the center of mass, and is not directly affected by confinement within pores larger than 20 Å. However, it is reasonable to presume that confinement affects the rotational dynamics through translational–rotational coupling. In this case the pore dimensions are quite similar and we do not find any clear evidence of this effect. In Fig. 7(b) the continuous line represents a linear fit to the eight points. The investigated temperature range is too small to analytically study the temperature dependence of the dynamical parameters. We are collecting data at lower and higher temperatures in order to address this question.

We can now compare the average translational and rotational relaxation times of water in these MCM matrices with those of bulk water at the same temperature. As far as the translational dynamics is concerned, we compare the self-diffusion constant of water as found using QENS and nuclear magnetic resonance (NMR).^{20,21} However, in the RCM the translational α relaxation is not described in terms of a diffusion coefficient. Nevertheless, we find $\gamma \approx 2$ at $T = 280$ K in both samples. Thus, in this case, we can define a translational diffusion coefficient, $D = a^2/\langle\tau_0\rangle$. At $T = 280$ K, in bulk water²² $D = 1.39 \times 10^{-5}$ cm²/s, we find $D = 3.24 \times 10^{-6}$ cm²/s in the MCM-41-S sample and $D = 2.79 \times 10^{-6}$ cm²/s in the MCM-48-S sample, with an effective slowing down of the translational dynamics by a factor of 4 and 5 times, respectively. It is also interesting to compare these findings with the results of a previous work on water confined in a Vycor glass with average pore diameter of 50 Å, in which the data have been analyzed using the translational RCM.¹ We simply compare the average translational relaxation times at $Q = 0.46 \text{ \AA}^{-1}$, at this low Q value rotational contributions are negligible. In Vycor $\langle\tau_T\rangle$ ($Q = 0.46 \text{ \AA}^{-1}$) = 82.43, 109.49, and 158.41 ps, at $T = 278$, 268, and 258 K, respectively. In MCM-41-S we find $\langle\tau_T\rangle$ ($Q = 0.46 \text{ \AA}^{-1}$) = 145.7, 181.5, and 226.0 ps, in MCM-48-S we find $\langle\tau_T\rangle$ ($Q = 0.46 \text{ \AA}^{-1}$) = 159.8, 204.3, and 230.8 ps at $T = 280$, 270, and 260 K, respectively. Thus, in these MCM matrices, whose pore diameters are half of that of Vycor glass, the translational dynamic of water is, depending on temperature, about two times slower than that of water in vycor. These findings show that the translational dynamics of water is strongly slowed down in pores with such small dimensions.

As far as the rotational dynamics is concerned, it is well known that the characteristic relaxation time of the second-order rotational correlation function, τ_2 , is directly related to the NMR quadrupole relaxation time of deuterium or oxygen-17 nuclei in water.²³ We fitted the long-time part of the second-order rotational correlation functions, as determined from $C_1(t)$ using the maximum entropy method, with a stretched exponential function, $\exp[-(t/\tau_2)^{\beta_2}]$. Thus, we calculated the average relaxation time, $\langle\tau_2\rangle = (\tau_2/\beta_2)\Gamma(1/\beta_2)$. In bulk water it has been found²⁴ $\tau_{\text{NMR}} = \tau_2 = 4.82$, 7.04, and 11.3 ps at $T = 278$, 268, and 258 K, respectively. In MCM-41-S we find $\langle\tau_2\rangle = 8.4$, 29.9, and 45.0 ps, in MCM-48-S we find $\langle\tau_2\rangle = 10.9$, 24.5, and 37.4 ps at $T = 280$, 270, and 260 K, respectively. The rotational dynamics of water in these mesoporous matrices are from three to five times slower than that of bulk water, depending on

temperature. However, as compared with the translational dynamic, the rotational relaxation time is less affected by confinement. This result supports the idea that the rotational process is not directly influenced by constraints effective on a length scale of 20 Å.

MD simulations have shown that because of the translation-rotation coupling, the long-time part of the rotational correlation functions coincides with the translational ISF at a certain Q^* value. We have determined Q^* from the extracted values of τ_0 and τ_R , $Q^* = (1/a) (\tau_0/\tau_R)^{1/\gamma}$, and we report the results in Fig. 7, plot (c), as a function of temperature. For both samples it takes values close to 0.6 \AA^{-1} from $T=250$ to 270 K, and it slightly increases at $T=280$ K. MD simulations results on bulk supercooled water suggest that Q^* is temperature independent. Our findings could support this idea; in fact, the slightly higher value of Q^* found at $T=280$ K is within experimental uncertainties. On the other hand, we find Q^* values smaller than those obtained using MD simulations. Discrepancies with MD simulations, although small, can be connected with confinement effects. $(Q^*)^{-1} = 0.6^{-1} \text{ \AA} = 1.67 \text{ \AA}$ represents a characteristic length scale at which translational and rotational diffusions are strongly coupled. It is interesting that this characteristic length scale is of the order of a water molecule dimension, and it is roughly the distance that a water molecule must travel in order to break the cage of its neighbors, through a cooperative rearrangement of the cage itself.

V. CONCLUSION

In summary, using 6 Å neutrons and a high-resolution neutron spectrometer we have been able to study the single particle dynamics of interfacial water in MCM-41-S and MCM-48-S over a range of supercooled temperatures, just above the freezing points. We analyzed the QENS data using the relaxing cage model, which takes into account the consecutive effects of the initial trapping of a typical water molecule inside the cage of its neighbors and the subsequent relaxation of the cage, on the translational and rotational dynamics of the water molecule itself. We have been able to: (a) extract the fraction of water molecules, p , whose dynamics is much slower than that in the inner part of the pores; (b) determine the average relaxation times of the translational and rotational dynamics, $\langle \tau_0 \rangle$ and $\langle \tau_R \rangle$; (c) put into evidence that both these relaxations are not simple Debye processes; and (d) find out that, on lowering the temperature, the dimensionality of the diffusion process decreases, as shown by the Q dependence of the average translational relaxation time. From the average translational and rotational relaxation times we then calculated the value of the characteristic length scale, $(Q^*)^{-1}$, at which the translational and rotational diffusions are strongly coupled.

ACKNOWLEDGMENTS

We are grateful to Francesco Sciortino for providing us with an SPC/E water simulation package and for instructions on how to use the package. Research at MIT is supported by DE-FG02-90ER45429 and 2113-MIT-DOE-591. This work utilized facilities supported in part by the National Science Foundation under Agreement No. DMR-0086210. Identifica-

tion of a commercial product does not imply recommendation or endorsement by the National Institute of Standards and Technology, nor does it imply that the product is necessarily the best for the stated purpose.

APPENDIX: SPC/E SIMULATION

We carried out simulations, in an NVE ensemble, of 216 and 1000 water molecules contained in a cubic box of an edge 18.65 and 31.04 Å, respectively. The effective potential used is the extended simple point charge model SPC/E. This potential treats a single water molecule as a rigid set of point masses with an OH distance of 0.1 nm and a HOH angle equal to the tetrahedral angle 109.47° . The point charges are placed on the atoms and their magnitudes are $q_H = 0.4238e$ and $q_O = -2q_H = -0.8476e$. Only the oxygen atoms in different molecules interact among themselves via a Lennard-Jones potential, with the parameters $\sigma = 0.31656$ nm and $\epsilon = 0.64857$ kJ/mol. The interaction between pairs of molecules is calculated explicitly when their separation is less than a cutoff distance r_c of 2.5σ . The contribution due to Coulomb interactions beyond r_c is calculated using the reaction-field method, as described by Steinhäuser.²⁵ Also, the contribution of Lennard-Jones interactions between pairs separated by more than r_c is included in the evaluation of thermodynamic properties by assuming a uniform density beyond r_c . A heat bath²⁶ has been used to allow for heat exchange. In our simulation, periodic boundary conditions are used. The time step for the integration of the molecular trajectories is 1 fs. The trajectories are generated up to 10 ns range, long enough to cover the slow relaxational times of both the translation and rotation. Simulations at low T were started from equilibrated configurations at higher T . Equilibration was monitored via the time dependence of the potential energy. In all cases the equilibration time t_{eq} was longer than the time needed to enter the diffusive regime. We studied three temperatures, 284.5, 250.0, and 225.0 K. We note that for the SPC/E model of water, the density maximum occurs at about 250 K, which corresponds to 277 K in the real water. Further detailed thermodynamic parameters of the simulations are given in previous papers.^{19,27} The SPC/E potential has been explicitly parametrized to reproduce the experimental value of the self-diffusion constant at ambient temperature and at a density of 1 g/cm^3 .²⁶

¹J. M. Zanotti, M.-C. Bellissent-Funel, and S.-H. Chen, Phys. Rev. E **59**, 3084 (1999).

²S.-H. Chen, C. Liao, F. Sciortino, P. Gallo, and P. Tartaglia, Phys. Rev. E **59**, 6708 (1999).

³L. Liu, A. Faraone, and S.-H. Chen, Phys. Rev. E **65**, 041506 (2002).

⁴P.-C. Shih, H.-P. Lin, and C.-Y. Mou, Chem. Mater. (to be published).

⁵Y. Liu, W. Zhang, and T. J. Pinnavaia, J. Am. Chem. Soc. **122**, 8791 (2000).

⁶J. R. D. Copley and J. C. Cook, Chem. Phys. (to be published).

⁷V. Crupi, D. Majolino, P. Migliardo, and V. Venuti, J. Phys. Chem. B **106**, 10884 (2002).

⁸M.-C. Bellissent-Funel, S.-H. Chen, and J. M. Zanotti, Phys. Rev. E **51**, 4558 (1995).

⁹P. Gallo, M. Rovere, and E. Spohr, Phys. Rev. Lett. **85**, 4317 (2000); J. Chem. Phys. **113**, 11324 (2000).

¹⁰E. Fratini, S.-H. Chen, P. Baglioni, and M.-C. Bellissent-Funel, Phys. Rev. E **64**, 020201 (2001).

¹¹A. Faraone, S.-H. Chen, E. Fratini, P. Baglioni, L. Liu, and C. Brown, Phys. Rev. E **65**, 040501 (2002).

- ¹²S.-H. Chen, P. Gallo, and M.-C. Bellissent Funel, *Can. J. Phys.* **73**, 703 (1995).
- ¹³S.-H. Chen, P. Gallo, F. Sciortino, and P. Tartaglia, *Phys. Rev. E* **56**, 4231 (1997).
- ¹⁴D. Di Cola, A. Deriu, M. Sampoli, and A. Torcini, *J. Chem. Phys.* **104**, 4223 (1996).
- ¹⁵V. F. Sears, *Can. J. Phys.* **45**, 237 (1967).
- ¹⁶L. Fabbian, F. Sciortino, and P. Tartaglia, *J. Non-Cryst. Solids* **235–237**, 325 (1998).
- ¹⁷B. J. Berne, P. Pechukas, and G. D. Harp, *J. Chem. Phys.* **49**, 3125 (1968).
- ¹⁸We are going to report the results of these measurements in a future paper.
- ¹⁹F. Sciortino, P. Gallo, S.-H. Chen, and P. Tartaglia, *Phys. Rev. E* **54**, 6331 (1996).
- ²⁰J. Teixeira, M.-C. Bellissent-Funel, S.-H. Chen, and A. J. Dianoux, *Phys. Rev. A* **31**, 1913 (1985).
- ²¹F. X. Prielmeier, E. W. Lang, R. J. Speedy, and H. D. Lüdemann, *Ber. Bunsenges. Phys. Chem.* **92**, 1111 (1988).
- ²²S.-H. Chen, in *Hydrogen Bonded Liquids*, Vol. 329 of *NATO Advances Study Institute, Series C: Mathematical and Physical Sciences*, edited by J. C. Dore and J. Teixeira (Kluwer Academic, Dordrecht, 1991).
- ²³E. W. Lang, H. D. Lüdemann, and L. Piculell, *J. Chem. Phys.* **81**, 3820 (1984).
- ²⁴E. Lang and H. D. Lüdemann, *Ber. Bunsenges. Phys. Chem.* **84**, 462 (1980); **85**, 603 (1981).
- ²⁵O. Steinhauser, *Mol. Phys.* **45**, 335 (1982).
- ²⁶H. J. C. Berendsen, J. P. M. Postma, W. F. van Gunsteren, A. Di Nola, and J. R. Haak, *J. Chem. Phys.* **81**, 3684 (1984).
- ²⁷P. Gallo, F. Sciortino, P. Tartaglia, and S.-H. Chen, *Phys. Rev. Lett.* **76**, 2730 (1996).